ORIGINAL ARTICLE

Quantification of tooth displacement from cone-beam computed tomography images

Jie Chen,[a] Shuning Li,[b] and Shiaofen Fang[c]
Indianapolis, Ind

Introduction: The objectives of this study were to demonstrate a method that could be used to quantify three-dimensional (3D) tooth displacement from cone-beam computed tomography (CBCT) images and to assess its accuracy. **Methods:** Images of the same mandible taken 2 weeks apart with no treatment were used. Four mandibular teeth—left lateral incisor, left canine, left first premolar, and left first molar—either remained unmoved or were artificially displaced with known values on 1 image to simulate after-treatment conditions. The iterative closest point method was used to superimpose the unchanged bony part of the mandible and to find the transformation matrix between a tooth's 2 positions, before and after displacement. Tooth displacement was calculated from the transformation matrix. **Results:** All 6 displacement components in terms of translations along and rotations about the 3 axes on the tooth were obtained. The results showed that the errors could be managed: they were less than 5% in translation and 10% in rotation. **Conclusions:** The 3D tooth displacement can be obtained from CBCT images, and the accuracy is acceptable for clinical use and can be improved when the quality of the images improves. (Am J Orthod Dentofacial Orthop 2009;136:393-400)

In orthodontics, patients are treated by moving teeth to improve esthetics and occlusion. Tooth displacement is an important outcome, which can be used to evaluate treatment strategies and orthodontic appliances. However, quantification of clinical 3-dimensional (3D) tooth displacement has been a major challenge.

Two-dimensional tooth displacement has been mostly evaluated clinically with panoramic and cephalometric radiographs.[1,2] Dental implants were used as radiographic landmarks to quantify the displacement of mandibular molars.[3] Only a projection of the displacement in the 2-dimensional plane could be measured; thus, the coupling effects (displacement perpendicular to the plane) were not measurable. Resent studies have focused on 3D displacement after orthodontic treatment.[4-13] The displacement was calculated based on displacements of a few points measured by a 3-axis measuring microscope[11] or surface points on the crown from digital dental casts.[4-10,12] The challenges are to locate the points consistently and accurately for the former and to reduce errors while making and digitizing the casts for the latter. The 3D displacement needs to be described relative to unchanged anatomic markers. Teeth were not the candidates because they might move. Thus, other anatomic regions, such as rugae[4-7,12] or implants have been used.[7,8,10,12] The position of the implants or the profile of the landmarks was recorded by impressions and corresponding dental casts. The casts were either scanned or digitized into a computer to create digital casts. Tooth displacements were calculated from the digital casts. The disadvantages are that implants are invasive, and the dental cast might not be accurate because the many steps in making a cast can introduce cumulative errors. It is clinically preferable if the 3D tooth displacement can be quantified in a less invasive and more accurate manner.

Cone-beam computed tomography (CBCT) is increasingly used in clinics as a means to obtain a digital jaw model. It has been used to quantify displacement of the condyles and the rami.[14,15] Its resolution has been improved and has the potential to be even better. Thus, it can be used to reliably reconstruct bone and teeth at different times; this is crucial for quantification of tooth displacement.

Our objectives in this study were to demonstrate a method to calculate 3D tooth displacements from CBCT images and to estimate their variations. These will pave the way for 3D tooth displacement quantification in the clinic.

From Indiana University Purdue University, Indianapolis, Indianapolis, Ind.
[a] Professor, Departments of Mechanical Engineering and Oral Facial Development.
[b] Graduate student, Department of Mechanical Engineering, Indiana University Purdue University, Indianapolis, Indianapolis, Ind.
[c] Associate professor, Department of Computer Science, Indiana University Purdue University, Indianapolis, Indianapolis, Ind.
This study was partially supported by a grant from Indiana 21st Century Fund and NIH-NIDCR R41-DE017025.
The authors report no commercial, proprietary, or financial interest in the products or companies described in this article.
Reprint requests to: Jie Chen, Department of Mechanical Engineering, 723 W Michigan St, Indianapolis, IN 46202; e-mail, jchen3@iupui.edu.
Submitted, June 2007; revised and accepted, October 2007.
0889-5406/$36.00

doi:10.1016/j.ajodo.2007.10.058

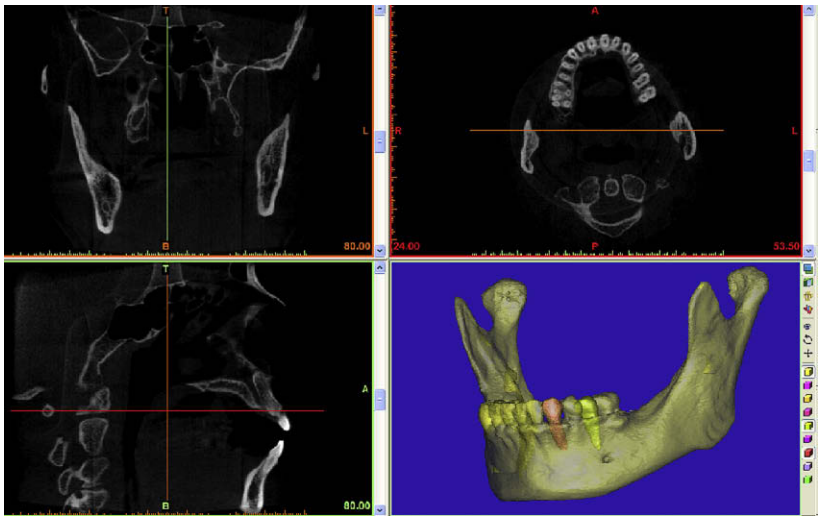

Fig 1. CBCT images of the volunteer and the mandible extracted from the 3D CBCT images.

MATERIAL AND METHODS

CBCT (i-CAT, Imaging Science International, Hatfield, Pa) records of an adult volunteer previously made for another purpose were used. Each scan took 40 seconds and had a voxel size of 0.25 mm (Fig 1). The dose was about 200 μSv. The volunteer was scanned twice 2 weeks apart with no orthodontic treatment, so that negligible tooth movement was expected. The use of the records was approved by the institutional review board of Indiana University.

Bone and teeth were reconstructed by using the MIMICS image processing software (Materialise Group, Leuven, Belgium). The cross sections of the CBCT images were carefully examined first. Human intervention was needed when clear boundaries of a root were not observed on the cross sections. The boundaries were manually reconstructed by using the tools in the MIMICS software. The segmentation function was used, first, to isolate the mandible from the rest of the tissues and, then, to separate the teeth from the bone. Individual tooth and bone models were created that were distinguishable by assigned colors (Fig 1).

Two mandible models were created from the 2 sets of CBCT images. The first set was considered as before treatment (BT) and the second as after treatment (AT1) with no tooth displacement. A third model (AT2) was created by artificially displacing certain teeth of the AT1 to simulate displacements from orthodontic treatment. The teeth were digitally displaced individually by using the MIMICS software with prescribed displacements on its assigned body coordinate system (Fig 2). The displacement included a translation along an axis and rotations about any of the axes. The 3 models were exported for calculating the tooth displacements.

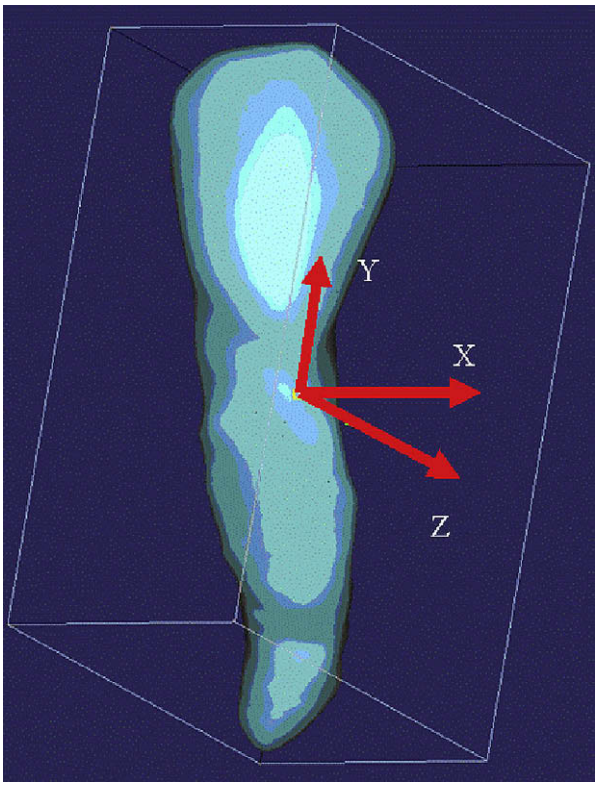

Fig 2. A MIMICS-assigned coordinate system was established on the left mandibular canine. Similar coordinate systems were assigned to the other 3 teeth.

The 3D displacement was expressed in the rectangular coordinate system on the tooth. It had 6

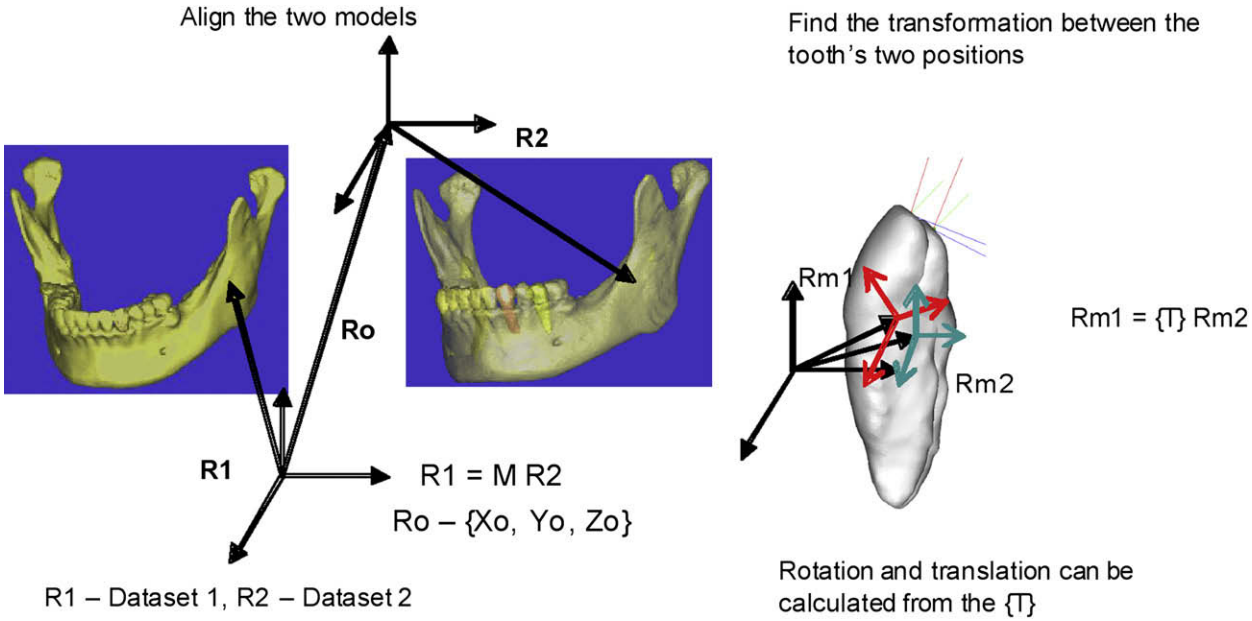

Fig 3. Scans of the before and after tooth displacements can be overlapped with the ICP. The *white tooth model* shows the 2 positions of the left canine. The scans are expressed in their own cooridinate systems, *R1* and *R2*. The transformation (*M*) between the 2 systems can be determined by using the data sets of the unchanged bony regions on the mandible, which overlaps in the 2 scans. Local coordinate systems, *Rm1* and *Rm2*, are created on the tooth's 2 positions. Then, transformation (*T*) is computed also with the ICP for determining rotation and translation of the tooth.

components: 3 translational and 3 rotational. In this study, displacements of 4 teeth—left lateral incisor, left canine, left first premolar, and left first molar—were calculated, each representing its own category so that the effects of tooth complexity on the calculated displacement could be assessed. Each tooth had its own coordinate system assigned by MIMICS (Fig 2). The prescribed tooth displacement was on this coordinate system.

Calculation of displacement was based on the tooth in its 2 positions. The positions could be identified by overlapping the unchanged portion of the 2 digital models (Fig 3). The basis of the overlapping technique is a geometric optimization algorithm, iterative closest point (ICP),[16] which precisely aligns the 3D polygon mesh data sets of the digital models. The main purpose is to be able to use unchanged anatomic structures (eg, a portion of the unchanged bone in the CBCT scan) as the reference to quantify tooth displacements.

When a mandible is scanned many times after different levels of tooth displacements, the common references of the scanned digital forms (data sets) need to be aligned precisely to allow meaningful comparisons and displacement measurements. An alignment can be made by using more than 3 landmark points that are manually selected on the models. This alignment, however, is not accurate, since small errors in detecting the coordinates of the landmark points will lead to significant errors in the resulting alignment. To achieve precise alignment, in this study, all surface data points (>600) in the static region were used. The data set was defined by a cylindrical primitive with its long axis vertical in Figure 4, *A*. The diameter of the cylinder was large enough to cover the lower portion of the mandible. The covered volume is shown by the shielded areas in Figure 4, *A*. The data points in 2 images were aligned by applying the ICP algorithm to overlap the 2 mandibles (Fig 4, *B*). The algorithm has been widely used in face recognition to align facial images.[16,17]

The ICP algorithm works as follows: from two 3D point sets, it finds the transformation that brings 1 data set into the best possible alignment with the other data set. The algorithm is to compute the optimal transformation (M) by iteratively finding a local minimum of a mean-square distance metric (Fig 3). In this implementation, the cost function is defined as the mean of the least-square distances from the vertices of 1 data set to the other:

$$f(M) = \frac{1}{N}\sum_{i} \|x_i - Mp_i\|^2$$

where M is a rigid transformation matrix, N is the number of points, x_i is the vertex of the first data set, and p_i is

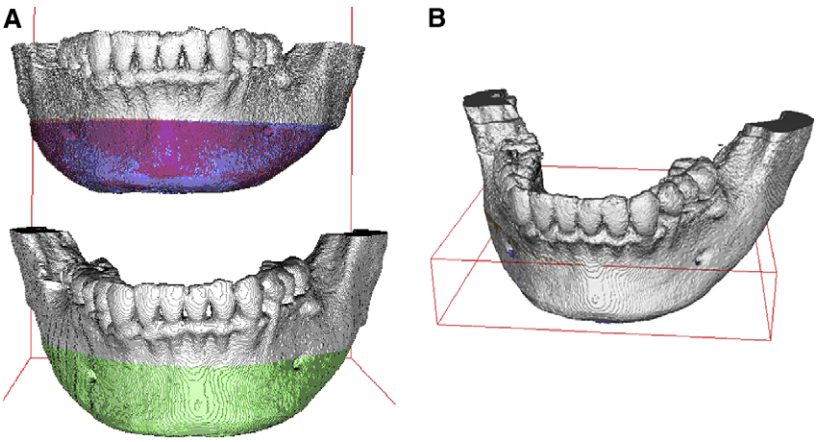

Fig 4. A, The mandible was scanned twice and reconstructed by using MIMICS.The *colored areas* were enclosed by a cylindrical primitive and were used to align the 2 images; **B,** the 2 mandibles were overlapped by using the ICP based on the alignment of the bone in the primitive (*red frame*).

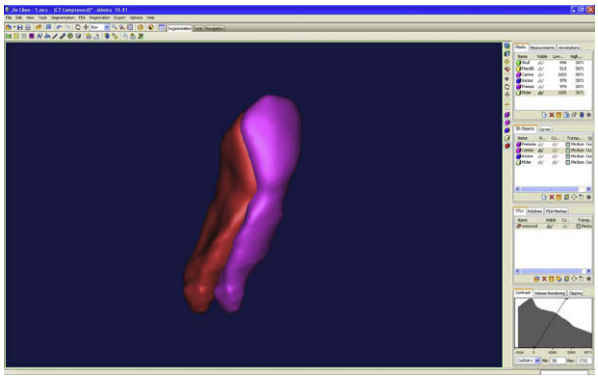

Fig 5. The right mandibular canine is displaced 2 mm along the z-axis and rotated 5° about the same axis. The transformation matrix between the 2 positions of the tooth is calculated by selecting the data sets at the positions and using the ICP.

the vertex of the second data set that is the closest to x_i. This process converges when the mean squared error stops improving. The optimal transformation produces the minimum mean squared error that measures the difference of the 2 data sets in consecutive steps. The transformation matrix, M, between the data sets in 2 positions is the accumulative matrix calculated from the matrices of every step. The 2 data sets are best aligned by using the M.

In orthodontics, teeth move, but the bone shape away from the teeth has negligible change in an adult. To relate a tooth's 2 positions, the subsets (bony part) of the scanned data sets that are unchanged after tooth movement are aligned. The 2 subdata sets generally produce an accurate alignment because the unchanged portion dominates the optimization process. The transformation matrix, M, is used to align the 2 models.

Table I. Prescribed tooth displacements of the 4 cases for the 4 teeth on AT2

Case	*Translation along*	*Rotation about*
1	z: 2.00 mm	z: 5.0°
2	z: 2.00 mm	z: 5.0°
		x: 5.0°
3	z: 2.00 mm	z: 5.0°
		y: 5.0°
4	z: 2.00 mm	x: 5.0°
		y: 5.0°

After the alignment, the 2 positions of the moving tooth are identifiable (Fig 5). The transformation between the 2 positions can be calculated by using the entire surface points on the tooth; this is accurate, robust, and easy to implement. Then the tooth displacement's 6 components in terms of translation along and rotation about the 3 coordinate axes of the BT model can be calculated from the entries of the transformation matrix.[18]

The usability of the method depends on its accuracy and variation. Experiments were designed to assess the errors and variations caused by various noises. The accumulative errors were assessed by comparing calculated tooth displacements with the prescribed values.

Two experiments were performed. The tooth displacements, from BT to AT1 and from BT to AT2, were known. The prescribed displacements were zero for AT1 and are shown for AT2 in Table I. Four displacement cases with different angle combinations prescribed to AT2 on the MIMICS-assigned tooth coordinate system were tested. The first case included translation of 2 mm

Table II. Means and standard deviations of the 5 repeats for calculating the displacements of the 4 teeth on AT1

	1	*2*	*3*	*4*	*5*	*Mean (mm)*	*SD*
Incisor							
T (mm)	0.09	0.02	0.04	0.07	0.06	0.06	0.03
R (°)	0.81	0.00	0.00	0.81	0.00	0.32	0.44
Canine							
T (mm)	0.01	0.02	0.01	0.00	0.00	0.01	0.01
R (°)	0.00	0.00	0.00	0.00	0.00	0.00	0.00
Premolar							
T (mm)	0.03	0.02	0.02	0.03	0.03	0.03	0.00
R (°)	0.00	0.00	0.00	0.00	0.00	0.00	0.00
Molar							
T (mm)	0.10	0.10	0.14	0.07	0.07	0.10	0.03
R (°)	0.00	0.81	0.00	0.81	0.81	0.49	0.44

T, Translation; *R,* rotation.

along the z-axis and rotation of 5° about the z-axis (Fig 2). For all other cases, translation of 2 mm along the z-axis and rotations of 5° about different axes were introduced. The cases helped to estimate the errors of this method. The difference between the calculated tooth displacement and the prescribed value was the error. The first experiment was used to assess the accuracy and the second to assess the percentage of the errors.

To assess the variation, the process of obtaining tooth displacements was repeated 5 times by one investigator (S.L.). For the displacement between BT and AT1, the process was repeated; for the rest of the cases, the process started after tooth segmentation because that was done before the AT2 model was made. The filters and thresholding values were identical. The means and standard deviations were computed to determine the accuracy and variation of the method.

RESULTS

The process-related variations were assessed for the 4 teeth. The means and standard deviations from the 5 repeats for the 2 experiments are shown in Tables II and III, respectively. With no prescribed displacement, the maximum calculated average translation and rotation were 0.10 mm (SD, 0.03 mm) and 0.49° (SD, 0.44°), respectively. The values were the errors because the prescribed displacements were zero. For the 2-mm prescribed translation, the average translations for the teeth were 2.01 mm for the incisor, 2.04 mm for the canine, 1.96 mm for the premolar, and 2.01 mm for the molar. For the 5° prescribed rotation, the average rotations for the teeth were 5.28° for the incisor, 5.10° for the canine, 5.13° for the premolar, and 5.26° for the molar. The standard deviations are also shown in Table III.

Percent error (PE) is a good indicator of accuracy and is evaluated by comparing calculated displacement (CD) to the prescribed displacement (PD) when PD is not zero. The PEs were calculated by the following formula:

$$PE = \left|\frac{CD - PD}{PD}\right|\%$$

The PE for each case in the second experiment is shown in Table IV; the PE varied among the cases. For the translations, the average PEs of all 4 cases were 0.74% for the incisor, 2.08% for the canine, 1.75% for the premolar, and 0.46% for the molar. For the rotations, the average PEs were 5.26% for the incisor, 1.95% for the canine, 2.57% for the premolar, and 5.25% for the molar, respectively.

DISCUSSION

A method has been developed to calculate tooth displacement from CBCT images. It involves extracting digital models of the mandible before and after displacement by using the segmentation method, overlapping the 2 models based on unchanged bony parts, and computing the 3D tooth displacements. In this article, only mandibular tooth displacement is presented.

For the model reconstruction, several techniques can be applied to a computed tomography (CT) image to reconstruct a geometric model of the teeth in the form of a dense polygon mesh surface. A popular technique is the marching cube based the iso-surface extraction algorithm.[19] Recent techniques can also be applied to help determine the proper iso-values for iso-surface definition.[20] Techniques for automatic or semiautomatic segmentation of tooth models from CT images have also been developed.[21] In this study, the MIMICS system was used for surface reconstruction and segmentation.

Table III. Means and standard deviations of the 5 repeats for calculating the displacements of the 4 teeth on AT2 corresponding to each case

	Direction	*1*	*2*	*3*	*4*	*5*	*Mean (mm)*	*SD*
Incisor								0.03
Case 1	Tz	2.01	1.98	1.98	2.02	2.05	2.01	
Case 2	Tz	2.02	1.97	1.98	2.02	2.04	2.01	0.03
Case 3	Tz	2.04	2.05	1.96	1.99	2.08	2.02	0.05
Case 4	Tz	2.13	1.85	1.82	2.10	1.98	1.98	0.14
Case 1	Rz	5.25	4.93	5.25	5.84	5.68	5.39	0.37
Case 2	Rz	5.06	4.93	4.87	4.8	4.66	4.86	0.15
	Rx	5.25	4.93	5.25	5.84	5.68	5.39	0.37
Case 3	Rz	5.19	5.06	5.01	5.06	5.73	5.21	0.30
	Ry	5.19	5.38	5.19	5.79	5.67	5.44	0.28
Case 4	Rx	4.50	5.56	4.67	5.89	5.13	5.15	0.63
	Ry	5.61	5.73	5.56	4.8	5.79	5.50	0.39
Canine								
Case 1	Tz	1.99	2.02	1.99	2.01	1.99	2.00	0.01
Case 2	Tz	1.98	1.99	2.00	2.01	1.98	1.99	0.01
Case 3	Tz	2.07	2.02	2.01	2.08	1.94	2.03	0.06
Case 4	Tz	2.07	2.17	2.10	2.03	2.37	2.15	0.13
Case 1	Rz	5.27	5.36	5.00	4.51	5.25	5.08	0.34
Case 2	Rz	5.19	4.73	5.32	5.1	5.13	5.09	0.22
	Rx	5.32	5.36	4.93	4.51	5.25	5.07	0.36
Case 3	Rz	5.4	5.56	5.11	4.73	5.31	5.22	0.32
	Ry	5.13	5.55	4.86	4.51	5.25	5.06	0.39
Case 4	Rx	5.37	5.56	5.26	5.4	4.58	5.23	0.38
	Ry	4.13	5.44	5.00	4.79	5.25	4.92	0.51
Premolar								
Case 1	Tz	2.00	1.96	1.95	1.94	1.95	1.96	0.02
Case 2	Tz	2.03	2.07	1.94	1.94	1.98	1.99	0.06
Case 3	Tz	2.05	2.06	1.97	1.98	1.97	2.01	0.04
Case 4	Tz	1.89	1.90	1.89	1.90	1.89	1.89	0.01
Case 1	Rz	5.56	4.89	5.17	5.23	5.32	5.23	0.24
Case 2	Rz	4.66	5.73	5.17	5.23	4.86	5.13	0.41
	Rx	4.93	4.89	5	5.23	5.32	5.07	0.19
Case 3	Rz	5.65	5.06	5.17	4.36	5.17	5.08	0.46
	Ry	4.86	4.89	4.66	5.23	5.19	4.97	0.24
Case 4	Rx	5.19	5.78	4.29	5.79	5.05	5.22	0.62
	Ry	5.23	5.19	5.89	5.23	4.59	5.23	0.46
Molar								
Case 1	Tz	1.89	2.03	1.98	2.08	1.97	1.99	0.07
Case 2	Tz	1.85	2.07	1.97	2.08	1.99	1.99	0.09
Case 3	Tz	2.08	1.97	2.02	2.07	1.99	2.02	0.05
Case 4	Tz	1.93	2.31	1.91	2.02	1.97	2.03	0.16
Case 1	Rz	5.62	4.8	5.23	5.84	5.1	5.32	0.41
Case 2	Rz	5.06	4.36	4.73	5.84	5.85	5.17	0.67
	Rx	5.62	4.8	5.28	5.84	5.1	5.33	0.41
Case 3	Rz	5.25	4.73	5.06	4.93	5.75	5.14	0.39
	Ry	4.96	5.06	5.78	5.84	5.1	5.35	0.43
Case 4	Rx	4.96	5.26	5.4	5.19	4.58	5.08	0.32
	Ry	5.25	5.36	5.73	5.43	5.5	5.45	0.18

Tz, Translation in the z-direction; *Rx,* rotation about the x-axis; *Ry,* rotation about the y-axis; *Rz,* rotation about the z-axis.

The calculated displacement is affected by noises inherent in the process. The following noises most likely result in variations: imaging, limited resolution, manual intervention during separation of the teeth, and algorithm-related errors. The process variation was assessed by repeating it 5 times on the same images. The maximum standard deviations were 0.16 mm for translation and 0.67° for rotation. Currently, displacements in the clinic have been described in millimeters and degrees. The variation is much smaller than 1 mm for translation and 1° for rotation; thus, it should be suitable to describe tooth displacement.

Table IV. Comparison between average experimental results and prescribed displacements for the 4 teeth on AT2

				Experiment results		*Error*	
		Translation (mm)	*Rotation (°)*	*Translation (mm)*	*Rotation (°)*	*Translation (%)*	*Rotation (%)*
Incisor	Case 1	z: 2.0	z: 5.0	z: 2.01	z: 5.39	z: 0	x: 8
	Case 2	z: 2.0	z: 5.0	z: 2.01	z: 4.86	z: 0	z: –3
			x: 5.0		x: 5.39		x: 8
	Case 3	z: 2.0	z: 5.0	z: 2.02	z: 5.21	z: 1	z: 4
			y: 5.0		y: 5.44		y: 9
	Case 4	z: 2.0	x: 5.0	z: 1.98	x: 5.26	z: –1	x: 5
			y: 5.0		y: 5.49		y: 10
Canine	Case 1	z: 2.0	z: 5.0	z: 2.00	z: 5.08	z: 0	x: 2
	Case 2	z: 2.0	z: 5.0	z: 1.99	z: 5.09	z: 0	z: 2
			x: 5.0		x: 5.07		x: 1
	Case 3	z: 2.0	z: 5.0	z: 2.03	z: 5.22	z: 1	z: 4
				y: 5.0	y: 5.06		y: 1
	Case 4	z: 2.0	x: 5.0	z: 2.10	x: 5.45	z: 5	x: 9
			y: 5.0		y: 5.02		y: 0
Premolar	Case 1	z: 2.0	z: 5.0	z:1.96	z: 5.23	z: –2	x: 5
	Case 2	z: 2.0	z: 5.0	z:1.99	z: 5.13	z: 0	z: 3
				x: 5.0	x: 5.07		x: 1
	Case 3	z: 2.0	z: 5.0	z: 2.01	z: 5.08	z: 0	z: 2
				y: 5.0	y: 4.97		y: –1
	Case 4	z: 2.0	x: 5.0	z: 1.89	x: 5.22	z: –5	x: 4
				y: 5.0	y: 5.23		y: 5
Molar	Case 1	z: 2.0	z: 5.0	z: 1.99	z: 5.32	z: 0	x: 6
	Case 2	z: 2.0	z: 5.0	z: 1.99	z: 5.17	z: 0	z: 3
				x: 5.0	x: 5.33		x: 7
	Case 3	z: 2.0	z: 5.0	z: 2.02	z: 5.14	z: 1	z: 3
				y: 5.0	y: 5.35		y: 7
	Case 4	z: 2.0	x: 5.0	z: 2.03	x: 5.08	z: 1	x: 2
				y: 5.0	y: 5.45		y: 9

The accuracy of the method was tested by comparing the calculated displacements with those prescribed. The maximum translational error was 0.37 mm in canine displacement, and the rotational error was 0.89° in premolar displacement; these resulted in the PEs of 18% and 18%, respectively (Table III). The errors were significantly reduced when the process was repeated 5 times. These repeats reduced the maximum errors among the 4 teeth to 5% and 10%, respectively (Table IV). Thus, repeating the same process many times increases accuracy.

Accuracy and variation do not depend on the tooth structure. Four teeth with different structures were tested. The standard deviations of the translational and rotational displacements did not favor any tooth (Tables II and III), meaning that they do not depend on the structural complexity of the teeth.

The accuracy of the method heavily relies on the quality of the tooth segmentation, which depends on the quality of the image. With current technology, it is challenging to separate the root from the bone consistently. The tooth model in this study had vague boundaries at certain cross sections. Human intervention was needed to manually separate them; this was time-consuming and introduced errors to the shape of the tooth. The accuracy of the method was affected because the calculation depended on the surface point locations. The errors can be reduced when the resolution of the CBCT scan improves. The accuracy of the method will be further improved if the separation is done automatically so that human errors are not involved. At present, accuracy can be maintained if the process of determining the displacements is repeated many times, and the control parameters remain the same.

There are limitations to using this technology. First, patients should not have metals near the moving tooth because they cause artifacts that are difficult to remove from the images. Second, significant bone growth should be avoided because bony parts are used as the common references. Thus, the method should be used on the permanent dentition or for short-term evaluations. Finally, CBCT imaging is invasive so that institutional review board approval is needed when this technology is used. Furthermore, images from only 1 subject were used in this study. The effects of interpersonal variation of the images on the results were not assessed.

CONCLUSIONS

It is feasible to quantify clinical 3D tooth displacement from CBCT data. The method provides sufficient accuracy to compute the displacement. Accuracy will improve when the quality of CT images improves or the process is repeated many times.

REFERENCES

1. Nanda RS. Biomechanics in clincal orthodontics. Philadelphia: W.B. Saunders; 1996.
2. Herman RJ, Currier GF, Miyake A. Mini-implant anchorage for maxillary canine retraction: a pilot study. Am J Orthod Dentofacial Orthop 2006;130:228-35.
3. Roberts WE, Arbuckle GR, Analoui M. Rate of mesial translation of mandibular molars using implant-anchored mechanics. Angle Orthod 1996;66:331-8.
4. Ashmore JL, Kurland BF, King GJ, Wheeler TT, Ghafari J, Ramsay DS. A 3-dimensional analysis of molar movement during headgear treatment. Am J Orthod Dentofacial Orthop 2002;121:18-30.
5. Cha BK, Choi JI, Jost-Brinkmann PG, Jeong YM. Applications of three-dimensionally scanned models in orthodontics. Int J Comput Dent 2007;10:41-52.
6. Commer P, Bourauel C, Maier K, Jager A. Construction and testing of a computer-based intraoral laser scanner for determining tooth positions. Med Eng Phys 2000;22:625-35.
7. Hayashi K, Araki Y, Uechi J, Ohno H, Mizoguchi I. A novel method for the three-dimensional (3-D) analysis of orthodontic tooth movement-calculation of rotation about and translation along the finite helical axis. J Biomech 2002;35:45-51.
8. Hayashi K, DeLong R, Mizoguchi I. Comparison of the finite helical axis and the rectangular coordinate system in representing orthodontic tooth movement. J Biomech 2006;39:2925-33.
9. Hayashi K, Hamaya M, Mizoguchi I. Simulation study for a finite helical axis analysis of tooth movement. Angle Orthod 2005;75:350-5.
10. Hayashi K, Uechi J, Murata M, Mizoguchi I. Comparison of maxillary canine retraction with sliding mechanics and a retraction spring: a three-dimensional analysis based on a midpalatal orthodontic implant. Eur J Orthod 2004;26:585-9.
11. Iwasaki LR, Haack JE, Nickel JC, Morton J. Human tooth movement in response to continuous stress of low magnitude [see comment]. Am J Orthod Dentofacial Orthop 2000;117:175-83.
12. Keilig L, Piesche K, Jager A, Bourauel C. Applications of surface-surface matching algorithms for determination of orthodontic tooth movements. Comput Methods Biomech Biomed Engin 2003;6:353-9.
13. Yoshida N, Koga Y, Saimoto A, Ishimatsu T, Yamada Y, Kobayashi K. Development of a magnetic sensing device for tooth displacement under orthodontic forces. IEEE Trans Biomed Eng 2001;48:354-60.
14. Cevidanes LH, Bailey LJ, Tucker SF, Styner MA, Mol A, Phillips CL, et al. Three-dimensional cone-beam computed tomography for assessment of mandibular changes after orthognathic surgery. Am J Orthod Dentofacial Orthop 2007;131:44-50.
15. Cevidanes LH, Styner MA, Proffit WR. Image analysis and superimposition of 3-dimensional cone-beam computed tomography models. Am J Orthod Dentofacial Orthop 2006;129:611-8.
16. Besl PJ, Mckay ND. A method for registration of 3-D shapes. IEEE Transactions on Pattern Analysis and Machine Intelligence 1992;14:239-56.
17. Lu X, Colbry D, Jain AK. Matching 2.5D scans for face recognition. Proceedings of the International Conference on Biometric Authentication (ICBA; 2004 Jul 15-17. Hong Kong, China: Springer; 2004. p. 30-6.
18. Siegler S, Chen J, Schneck CD. The three-dimensional kinematics and flexibility characteristics of the human ankle and subtalar joints—part I: kinematics. J Biomech Eng 1988;110:364-73.
19. Lorensen WE, Cline HE. Marching cubes: A high resolution 3D surface construction algorithm. In: Stone MC, editor. Proceedings of the 14th annual conference on computer graphics and interactive technigues; 1987 Jul 19-24; Los Angeles, CA. New York: ACM Press; 1987. p. 162-9.
20. Fang S, Adada M. Multi-scale iso-surface extraction for volume visualization. Int J Image Graph 2006;6:173-86.
21. Kondo TOS, Chuah JH, Foong KW. Robust arch detection and tooth segmentation in 3D images of dental plaster models. International Workshop on Medical Imaging and Augmented Reality (MIAR '01); 2001 Jun 10-12; Hong Kong, China. Washington, DC: IEEE Computer Society; 2001. p. 241.